New insight of geomorphology and landslide prone area detection using Digital Elevation Model(s)

M. Jaboyedoff
Quanterra, Lausanne, Switzerland

F. Baillifard
Crealp (Research Center on Alpine Environment), Sion, Switzerland

R. Couture
Geological Survey of Canada, Ottawa, On, Canada

J. Locat, & P. Locat
Laval University, Quebec City, Qc, Canada

ABSTRACT: Starting from the hypothesis that the structure of a rock mass influences its geomorphology, digital elevation models (DEM) permit analyzing simple descriptors of the topography, such as terrain slope angle, slope aspect, etc. Case studies of slope instability in the western Swiss Alps clearly indicate that the 3D-interpretation of the relief makes it possible to perform geomorphological characterizations and to detect instabilities. The use of terrain descriptors leads to hazard assessment by estimating for instance terrain slope, fault orientations and locations, mean topography and kinematic tests. The presented method proves a good preliminary hazard assessment method.

1 INTRODUCTION

Landslide hazard assessment can be improved by using new digital documents such as digital elevation models (DEM). Geographic Information System (GIS) and geo-referenced documents being more and more available, the geomorphologic theories and methods that were developed before the computer age are now being updated and improved. They yield new insights for landslide hazard assessment.

Slope processes and associated morphology were extensively studied during the last two centuries (Gilbert 1880, De La Noe & De Margerie 1888). Terrain slope is the first way to qualify the topography (Strahler 1950) and the basic information used for slope modeling (Young 1972). Terrain slope depends on many factors such as weathering and rock types (Young 1961). In rock slopes, joints play an important role on the slope shaping (Terzhaghi 1962, Scheidegger 1980, Selby 1982).

Slope stability is dependent on rock mechanical properties. On one hand, landslides in loose materials (for example in sand piles) are often located within a defined terrain slope angle range (Rautela & Thakur 1999). On the other hand, rock slope stability is strongly controlled by discontinuities that decrease rock strength.

Thus, the analysis of the topography reflects the mechanical and structural features of the slope (Locat et al., 2000). Digital elevation models (DEM) makes it possible to perform more detailed and systematic morphological analysis. Using the orientation of each single cell, a DEM can be represented by 3D shaded relief that displays one color for each dip and direction of dip. This kind of representation permits a very simple slope analysis providing quick information for slope hazard assessment. Different cases in the western Swiss Alps are presented.

2 METHODS

The following method allows calculating various DEM descriptors. They are mainly dedicated to rock slopes, but can be applied to landslides that develop in unconsolidated materials. The presented DEM descriptors are often indicators of slope instability.

2.1 Slope angle histogram

All the DEM cell slope angles can be computed in a slope angle histogram. A simple interpretation of slope angle histograms gives information about slope stability. In loose materials, comparison between terrain slopes and landslide locations gives information about slope angle and landslide sensitivity (Rautela & Thakur 1999).

Assuming that rock mass properties control partly the topography, the histogram of slope orientations gives information on either fault or joint orientation, or on mechanical properties and erosion processes. Histograms can be calculated either on all pixels of the DEM or on selected points, exactly like for a stereonet density diagram. Depending on the rock types, a limit below which angle of slope is stable can be determined for each different lithology.

2.2 3D topographic analysis

Three-dimensional topographic analysis is performed by computing the orientation of each single cell of the DEM. The result provides a 3D color shaded relief map combining both terrain slope angle and slope aspect (direction of slope) in one single document (Fig. 3). The computer program COLPTOP3D (Jaboyedoff & Couture 2003) uses this principle to analyze and represent the 3D color shaded relief map. The slope orientation is coded following the Hue-Saturation-Intensity (HSI) code. A dip direction and a slope angle define each color (Fig.1).

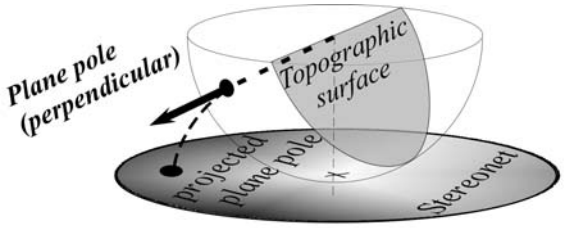

Figure 1. Principle of the color-coding represented in a lower Schmidt-Lambert stereonet (grayed scale replace colors).

This analysis makes it possible to identify the main structures (e.g. faults, joint sets, etc.) that shape the landscape, especially from a tectonic perspective. Also, this leads to the identification of the main potential sliding surfaces that can produce rockslides.

2.3 Fault traces and volumes

Once the discontinuity sets are identified and the areas shaped by them are detected, it is also possible to extend their traces by calculation using the COLTOP3D. This leads to the definition of potential unstable areas if the condition of sliding along faults or wedge is verified by kinematics tests. Several joints and fault traces can define a potential unstable volume.

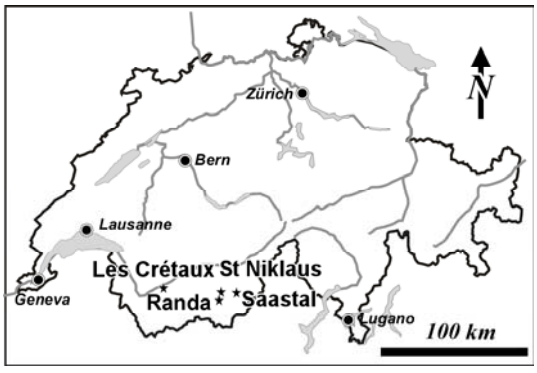

Figure 2. Location of the case studies.

2.4 Kinematic tests

The orientations of the main joint sets can be deduced from the analysis of the topography (see 2.1). The zones where instabilities can be produced by sliding or toppling on joint sets can then be deduced from the DEM automatic kinematic tests (Jaboyedoff et al. in press). This procedure checks if sliding or toppling conditions are verified (Gokceoglu et al. 2000, Günther 2003). Furthermore, the mean joint density can be estimated, giving information on the probability to find structures that could generate landslides (Jaboyedoff et al. in press).

2.5 Regional topography and residual topography

Regional topography is obtained by smoothing the topography that attenuates the spurs. Thus, the residual topography is defined as the difference between the original DEM and the smoothed DEM. Positive values are given to spurs and negative values to river valleys.

Spurs are often considered as more sensitive to instabilities (Dussauge-Peisser 2002). Thus the greater the residual value is, the bigger is the spur.

2.6 Combination of DEM descriptors

The above slope descriptors permit selection of landslide prone areas. Combination of descriptors is a simple way to select locations with higher hazard than other locations.

3 RESULTS

The use of the above-presented DEM descriptors is outlined using case studies in the western Swiss Alps.

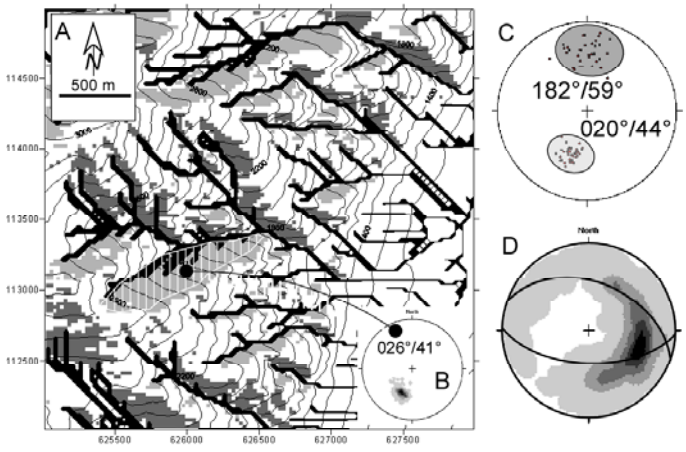

Figure 3. (A) Location of the areas oriented 182°/59° within a range of 30° (dark grey) and oriented 020°/44° within a range of 30° (light grey). Rivers are shown in black. The density stereonet (B) of all cells lying within the hatched area indicates a remarkable constancy in orientation. The stereonet (C) is produced by the COLTOP3D software, based on a series of selected points on the map showing the two main discontinuity

sets shaping the landscape. The stereonet (D) displays the river flow directions, compared with the orientations of the two main discontinuity sets (DHM25© 2004 swisstopo (BA045928)).

3.1 Large scale structural analysis in Mattertal

The western mountainside of the Mattertal (17 km north of Zermatt, in Switzerland) upstream from the village of St.Niklaus is made of a competent lithology, the Randa orthogneiss (Fig. 2). The 3D slope analysis demonstrates that the slope is mainly controlled by two large-scale discontinuity sets, confirmed by field surveys. These two sets (dip and dip direction are respectively 182°/59° and 020°/44°) are conjugated faults. Their acute intersection angle is 79° and the related wedge axis (i.e. intersection line) is approximately 100°/12°.

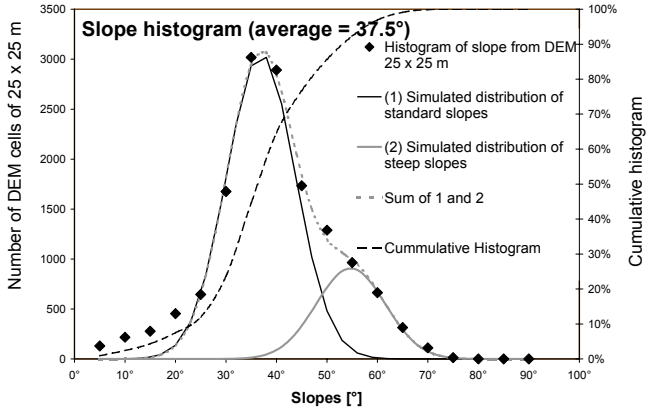

Figure 4. Histogram and modeling of slopes extracted from a 25 x 25 m DEM (modified after Rouiller et al., 1998).

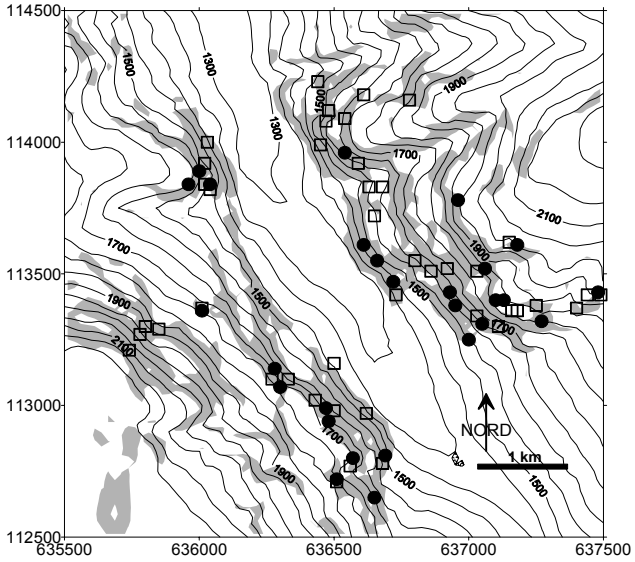

Figure 5. Map of a portion of the Saastal. The slopes steeper than 50° are shown in grey. Black dots represent the present rock instabilities and empty squares represent the ancient scars (modified after Rouiller et al. 1998).

The influence of faults and discontinuities on slope morphology has often been underlined by comparing polar histograms of rivers to polar histograms of joints (Scheidegger 1980). In the present case, the location of the virtual stream paths (calculated by standard GIS procedures) indicates that rivers follow mainly the two sets of discontinuities (Fig. 3). This is underlined by the density stereonet of the rivers orientation. The flow direction is mainly located within the wedges formed by the two conjugated fault sets and in the direction that belong to their great circles (Fig.3).

3.2 Example of slope analysis

Simple slope analysis was performed on a portion of the Saastal (Switzerland), within highly fractured orthogneisses, paragneisses, amphibolites and schist (Rouiller et al., 1998). The slope histogram shows clearly two gaussian populations that can be modeled (Fig. 4). The steepest one dominates for slopes steeper than 50°.

A detailed mapping of present rock instabilities and scars of ancient rockfalls clearly indicates that most of them are lying within the slopes that are steeper than 50° (Fig. 5). This indicates clearly a geomorphologic control on rock instabilities.

3.3 Les Crétaux landslide analysis

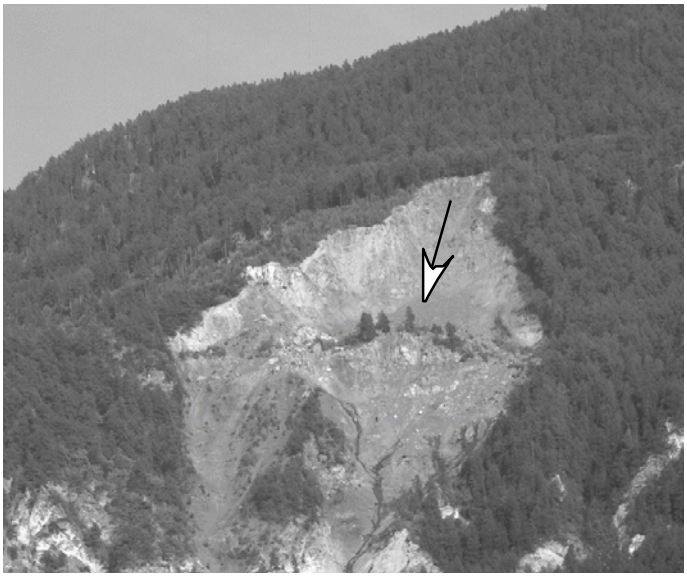

Figure 6. View to the southeast of the Les Crétaux landslide. The arrow indicates the displacement of the central rocky spur.

The rock instability of les Crétaux is located 10 km west of Sion, in Switzerland (Descoeudres & Zimmermann 1987). It developed in August 1985 in an ancient rock cliff. Blocks fell down from 1400 m in altitude to 450 m (Fig. 6). From that period on, around 800,000 m^3 have gradually moved down to the Rhône valley.

The 3D-analysis of the topography shows that the relief in the neighborhood of the rock instability is shaped by two faults: one dipping to the north

(006°/40°) and the other dipping to the west (282°/42°) (Fig. 7). The expected traces of the two discontinuities intersect below the moving rock mass, creating a wedge whose axis is oriented 330°/34°. That direction corresponds exactly to the observed mass movements.

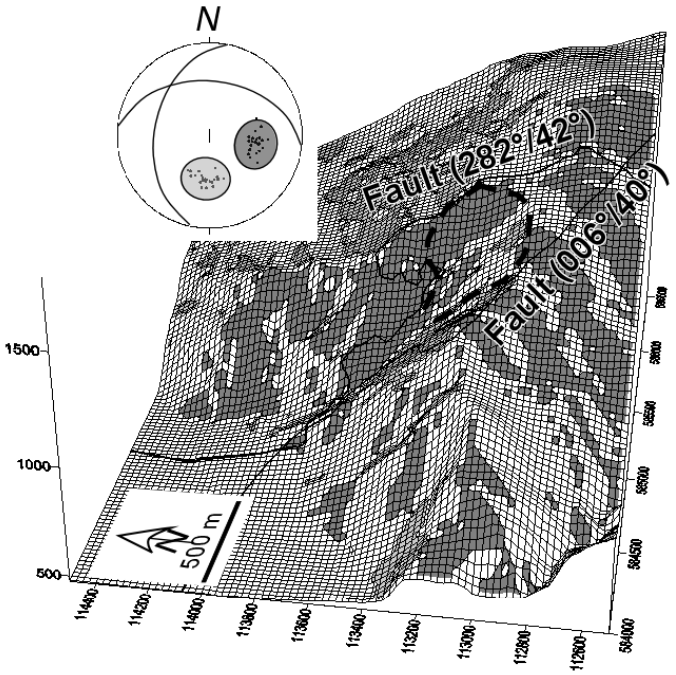

Figure 7. The dashed line indictes the location of the insatbility. The stereonet (lower hem.) indicate the data extracted from the DEM and used to determine the orientation of the faults. The two grey areas represent the two fault oreintations. The two expected faults are drawn on the topography (DTM reproduced with the permission of the Swiss Federal Service of the Topography, BA034918)

3.4 Randa rockfall: a back analysis

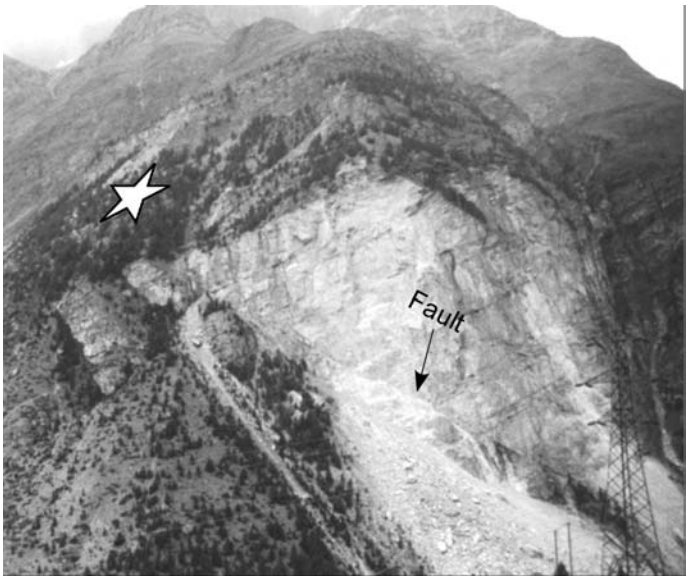

Figure 8. Photograph of the cliff at Randa, seven years before the rockfall. Note the basal fault J3 and its effect on the rock breakage (modified after Sartori et al. 2003).

About 30 million cubic meters of rocks fell from a rock face near the village of Randa (10 km north of Zermatt, Switzerland) in two main stages: the first one on April 18, 1991, and the second one on May 9, 1991. No fatalities were reported except for a few horses, cows and sheep. 31 chalets were buried, the road and the railway were destroyed. Structural analysis demonstrates that the Randa rockfall was mainly caused by a large discontinuity (Fig. 8) lying at the bottom of cliff and favoring its progressive breakage (Sartori et al. 2003).

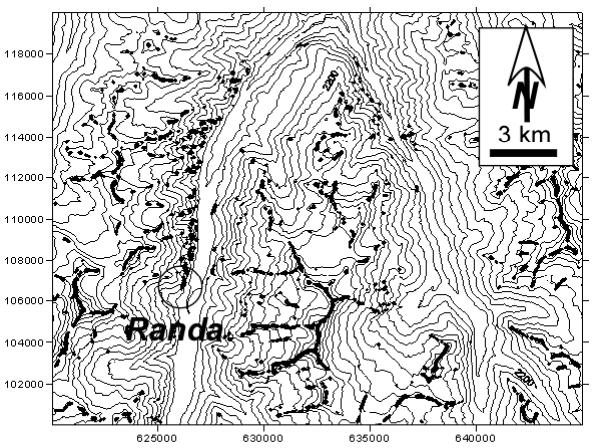

Figure 9. Map of the Randa area displaying the residual values over 50 m in black (Randa is about 140 m). Only limited zones are outlined by that method (DHM25© 2004 swisstopo (BA045928)).

The residual, based on a moving average of the DEM calculated in a square of 250 x 250 m, indicates that the Randa cliff possesses the highest values (Fig. 9) of the surrounding area (considering a 500 km^2-wide area including the Saastal and Mattertal). Moreover, the Randa cliff is the highest spur of the area. Note that the residual depends on the dimension of the moving average window.

The geomorphology within the Randa orthogneiss is largely controlled by faults. The 3D analysis of the relief permits definition of a very persistent fault set (J3) dipping on average 025°/33° that shapes the relief. This discontinuity set can be easily identified with COLTOP3D (Fig. 10). Its orientation corresponds to the basal sliding plane from the April 18 rockfall, that was oriented 030°/30° (Sartori et al. 2003).

J3 discontinuities are assumed to be potential sliding surfaces liable to produce rockfalls (Figs. 8, 11). An automatic kinematic test indicates the areas where sliding planes potentially daylight (Fig. 11). The Randa cliff possesses the highest average density of potentially dangerous J3 discontinuities.

The J3 morphological features can also be used to draw fault traces with J3-like orientation that are passing at the base of the outcrop. That way the hypothesis that large faults can affect the entire slope can be tested. The result indicates that some of the surfaces located south of Randa are potential con-

tinuation of the J3 basal fault that caused the April 18 rockfall.

Now comparing and using the indicators altogether, the Randa cliff appears to be a location that presents several unfavourable geomorphologic features that can be summarized as follows:

1. Steep slope
2. High value of 250 m moving average residual
3. High probability of potential sliding
4. Potential J3 discontinuity crossing the cliff

This back analysis shows clearly that the Randa rockfall is located in an area affected by a rockfall hazard among the highest in the surrounding region.

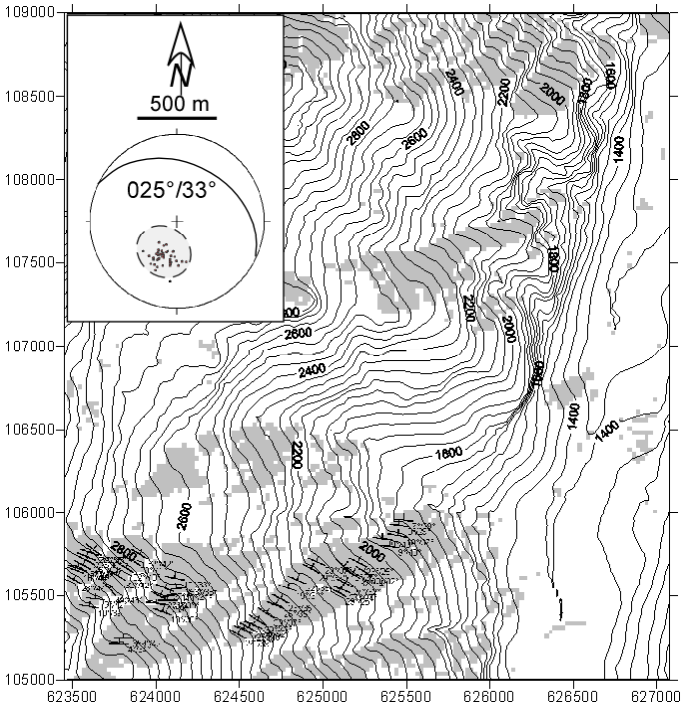

Figure 10. Topographic map of region surrounding the Randa rockfall. The relief orientations similar to J3 are displayed in grey (DHM25© 2004 swisstopo (BA045928)).

Based on the previous statements, the cliff situated north of the Randa cliff presents also a high hazard, displaying all the four parameters in the same location. Inspection of aerial photographs indicates that an ancient rockfall occurred at this location. The volume of the potential new instability is rather small, but it seems that this rock mass already moved recently. Field inspection will be necessary to observe if a J3 exists at the bottom of the cliff and if the stability of the cliff depends on J3 or not.

4 DISCUSSION

The use of DEM for landslide hazard assessment certainly permits to save money because it makes possible to perform a first level hazard assessment without any field investigation. It allows having a first identification of potential rockfall source areas presenting a high hazard, which will be a good guide for field investigations if needed.

The river orientations demonstrate that fracturing, especially high density fracturing associated with fault control erosion of rock slopes.

Slope angle analysis indicates that slope morphology is controlled by glacial erosion. Mountainsides displaying a U-shaped morphology show that the slope angles can be divide in two populations: (1) the steep slopes equivalent to the flank valley, and (2) the small slope angles occurring in the areas eroded by glaciers and suspended glaciers. The region of high curvature joining these two types of slopes is less represented in the slope histograms, which leads to two distinct populations.

The use of one or more descriptors is necessary to select potential unstable areas and/or to improve the results obtained with only one criterion such as slopes. By using the proposed descriptors, the Randa rockfall would have been detected, or the cliff would at least have been visited.

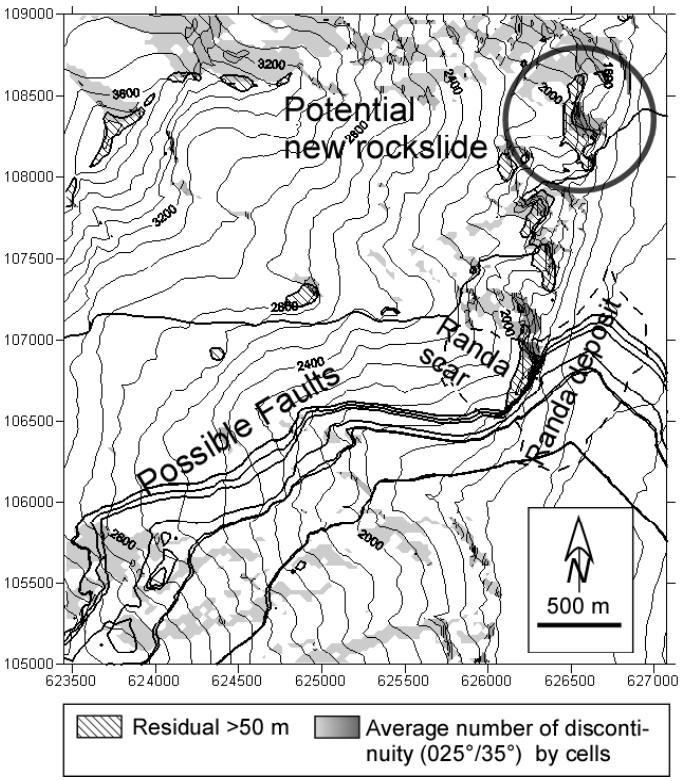

Figure 11. Topographic map around the 1991 Randa rockfall scar (dashed line). The greyed zones indicate the locations where J3 can produce slides; the darker the grey, the greater the chance to find a J3 discontinuity. The hatched perimeters correspond to high residuals. The expected fault traces are drawn. The three faults near to the 1991 scar are only represented in order to show that it is possible to find a fault that cuts the cliff at the position of the observed J3 discontinuity. Observe that all the different indicators are present in the Randa cliff. The circle indicates the area of potential future rockslide (DHM25© 2004 swisstopo (BA045928)).

It must be underlined that the mesh size of the DEM constraint the discontinuity detection. The sur-

face of the topography shaped by discontinuities must be larger than the mesh size.

5 CONCLUSION

3D-analysis of the relief permits to add a step in the slope hazard assessment. A preliminary study without any field investigations can be done very quickly, and new interpretations of instability mechanisms can be proposed. This is especially true when the large structures cannot be measured by field observations, because structures are too rare on the field. The increasing availability and precision of DEM will improve these methods.

Acknowledgments: The first author thanks the Société Académique Vaudoise for its grant and the EPFL for providing support. The second author is supported by the Swiss National Science Foundation (Grant Number 2100-50781.97). We thank Larry Dyke, from Geological Survey of Canada, for substantially improving our manuscript.

6 REFERENCES

De La Noe, G. & De Margerie, E. 1888. Du façonnement des versants. *Les formes du terrain* 3: 39-47.

Descouedres, F., & Zimmermann, Th. 1987. Three-dimensional dynamic calculation of rockfalls. *Proceedings 6th International Congress of Rock Mechanics. Montreal, Canada*: 337-342.

Dussauge-Peisser, C. 2002. *Evaluation de l'aléa éboulement rocheux. Développements méthodologiques et approches expérimentales. Application aux falaises calcaires du Y grenoblois,* PhD thesis, Université Joseph Fourier, Grenoble, France.

Gilbert, G. K. 1880. *Report on the Geology of the Henry Mountains*. U.S. Geographical and Geological Survey of the Rocky Mountain Region: 108-118.

Gokceoglu, C., Sonmez, H. and Ercanoglu, M. 2000. Discontinuity controlled probabilistic slope failure risk maps of the Altindag (settlement) region in Turkey. *Eng. Geol.* 55: 277-296.

Günther, A. 2003. SLOPEMAP: programs for automated mapping of geometrical and kinematical properties of hard rock hill slopes. *Computers & Geosciences* 29(7): 865-875.

Jaboyedoff, M., Baillifard, F., Philippossian, F. and Rouiller, J.-D., in press. Assessing fracture occurrence using "weighted fracturing density": a step towards estimating rock instability hazard. *Natural Hazards and Earth System Sciences* 4: 83-93.

Jaboyedoff, M. & Couture, R. 2003. Report on the project COLTOP3D for March 2003: stay of Michel Jaboyedoff at GSC - Ottawa . *Quanterra administrative document - Activity report - RA01*.

Locat, J., Leroueil, S. & Picarelli, L. 2000. Some considerations on the role of geological history on slope stability and estimation of minimum apparent cohesion of a rock mass. In Bromhead, E., Dixon, N. & M.L. Ibsen (eds) *Landslides in research, theory and practice. The 8th International Symposium on Landslides in Cardiff in the year 2000*. 935-942.

Rouiller, J.-D., Jaboyedoff, M., Marro, C., Philippossian, F. and Mamin, M., 1998. *Pentes intables dans le Pennique valaisan. Matterock: une méthodologie d'auscultation des falaises et de détection des éboulements majeurs potentiels.* Rapport final du PNR31. VDF, Zürich.

Rautela, P. & Thakur, V.C. 1999. Landslide hazard zonation in Kaliganga and Madhyamahshwar valleys of Garhwal Himalaya: A GIS basd approach. *Him. Geol.* 20(2): 31-44.

Sartori, M., Baillifard, F., Jaboyedoff, M. and Rouiller, J.-D., 2003. Kinematics of the 1991 Randa rockfall (Valais, Switzerland). *Natural Hazards and Earth System Sciences* 3(5): 423-433.

Scheidegger, E.A. 1980. Alpine joints and valleys in the Neotectonic stress-field. *Rock Mech.* Suppl. 9: 109-124.

Selby, M. J. 1982. Controls on the stability and inclinations of hillslopes formed on hard rock. *Earth Surface Processes and Landforms* 7: 449-467.

Strahler, A.N., 1950. Equilibrium theory of erosional slopes approached by frequency distribution analysis. *American Journal of Science* 248: 673-696, 800-814.

Terzaghi, K. 1962. Stability of slopes on hard unweathered rock. *Geotechnique* 12: 251-263.

Young, A. 1972. *Slopes*. Logman.

Young, A. 1961. Characteristic and limiting slope angles. *Zeitschrift fur Geomorphologie* 5: 126-131.